Rare Met. (2023) 42(1):146–154
https://doi.org/10.1007/s12598-022-02119-6

RARE METALS

ORIGINAL ARTICLE

Enhancing oxygen reduction reaction of Pt–Co/C nanocatalysts via synergetic effect between Pt and Co prepared by one-pot synthesis

Yun-Feng Wu, Ji-Wei Ma*, Yun-Hui Huang*

Received: 3 March 2022 / Revised: 18 April 2022 / Accepted: 22 April 2022 / Published online: 21 October 2022

Abstract Designing highly active and durable electrocatalysts towards oxygen reduction reaction (ORR) plays a paramount importance for proton exchange membrane fuel cells. Pt-based binary alloys Pt-M (M = 3d-transition metals) possessing excellent electronic and geometric properties have received increasing interests as highly active electrocatalysts. Herein, we report a series of Pt_xCo/C (x = 1, 2, 3) catalysts by a facile one-pot soft-chemistry method. In the acidic conditions, the mass activities of PtCo/C, Pt_2Co/C and Pt_3Co/C are 0.526, 0.462 and 0.441 $A{\cdot}mg_{Pt}{}^{-1}$, which are 2.60, 2.31 and 2.22 times higher than that of Pt/C (0.200 $A{\cdot}mg_{Pt}{}^{-1}$), respectively. The specific activities of PtCo/C, Pt_2Co/C and Pt_3Co/C are 706.59, 679.41 and 801.83 $\mu A{\cdot}cm^{-2}$, which are accordingly 2.89, 2.76 and 3.28 times higher than that of Pt/C (244.75 $\mu A{\cdot}cm^{-2}$). Notably, Pt_3Co/C shows a remarkable durability. After 5000 cycles of the accelerated durability testing, the mass activity and specific activity of Pt_3Co/C catalyst are 2.47 and 3.80 times higher than that of the commercial Pt/C, respectively. The improved ORR activity and durability can be ascribed to the synergistic interaction between Pt and Co.

Keywords Proton exchange membrane fuel cells (PEMFCs); Pt_xCo/C catalysts; Synergetic effect; Oxygen reduction reaction (ORR); One-pot synthesis

1 Introduction

Proton exchange membrane fuel cells (PEMFCs) are considered as highly potential energy convention devices without emission of pollution [1–3]. The challenge for PEMFCs is the poor kinetics of the cathodic reaction that is several orders of magnitude slower than that of the anodic reaction [4–7]. Platinum is an ideal catalyst to promote the kinetics of cathodic reaction, but its scarcity and high cost limit its wide applications [8–10]. Hence, it is important to develop Pt-based alloy electrocatalysts with less platinum and high performance. Current strategies usually focus on modifying the microstructures of the electrocatalysts to enhance activity and durability. For example, fabricating the microstructures, such as nanotubes [11], nanocages [12–14], nanowires [15–17], nanoframes [18–20] and nanodendrites [21, 22], can lead to more active sites and higher specific electrochemical surface area. Reducing the particle size of the catalysts can promote the utilization of Pt, which can enhance the mass activity (MA) and specific activity (SA). However, reducing the size will lead to the agglomeration of particles and further growth due to the Ostwald ripening [23–25]. Indeed, platinum has the superior ability to weaken the binding energy of the oxygen reduction reaction intermediates, which limits the kinetics of the cathodic reaction [26, 27]. To decrease the amount of Pt and improve the oxygen reduction reaction (ORR) activity, combining Pt

---

Supplementary Information The online version contains supplementary material available at https://doi.org/10.1007/s12598-022-02119-6.

Y.-F. Wu, J.-W. Ma*
School of Materials Science and Engineering, Tongji University, Shanghai 201804, China
e-mail: jiwei.ma@tongji.edu.cn

Y.-H. Huang*
School of Materials Science and Engineering, Huazhong University of Science and Technology, Wuhan 430074, China
e-mail: huangyh@hust.edu.cn

with some non-precious metals is an effective strategy to tune the ORR activity.

Previous reported results have demonstrated that alloying Pt with 3d transition metals such as Fe, Co and Ni will downshift the d-band state, which could change the electronic structure of Pt-based catalysts, promoting high ORR activity and durability [28–33]. Among various Pt-based alloys, Pt–Co catalysts are considered as promising ORR electrocatalysts due to high activity and reasonable durability [34, 35]. However, dispersing agents such as surface-active substances have been generally employed during the synthetic process, and it is hard to remove them in the post-treatment process [36, 37], which might have a negative effect on ORR activity. In addition, the prepared catalysts need to be loaded on carbon or other supports before electrochemical tests [38, 39]. Herein, we deployed a facile strategy via one-pot synthesis without adding surfactant to prepare a series of carbon-supported Pt_xCo (x = 1, 2, 3) catalysts. The particle size of as-prepared Pt_xCo/C catalysts was around 4 nm, and the shape of particles was uniform. All the as-prepared Pt_xCo/C (x = 1, 2, 3) catalysts showed improved ORR activity and durability compared to the commercial Pt/C catalyst. Notably, the Pt_3Co/C catalyst showed remarkable durability compared to the commercial Pt/C catalyst and its analogs (PtCo/C and Pt_2Co/C catalysts).

2 Experimental

2.1 Materials

Chloroplatinic acid hexahydrate ($H_2PtCl_6\cdot6H_2O$, Aladdin), cobalt chloride hexahydrate ($CoCl_2\cdot6H_2O$, Aladdin), ethylene glycol (EG, 99%, Aladdin), carbon black (EC300, Cabot Corporation), acetaldehyde (99%, Aladdin), Nafion (5%, Dupont), and ultrapure water (18.2 MΩ·cm, 25 °C) were used in the experiment.

2.2 Preparation of Pt_xCo/C catalysts

50 mg EC300 was scattered in 100 ml ultrapure water by ultrasonicating for 30 min till thoroughly dispersed. After that, 50 ml EG solution containing 120.5 mg $H_2PtCl_6\cdot6H_2O$, 18.5 mg $CoCl_2\cdot6H_2O$ and 0.2 $mmol\cdot L^{-1}$ acetaldehyde was added into the carbon solution suspension to form a mixed solution, which was then stirred for 1 h at 80 °C. The mixed solution was filtered, washed with ultrapure water and dried in oven, and finally, Pt_3Co/C catalyst was attained. At the same time, PtCo/C and Pt_2Co/C catalysts were attained via the same method only by varying the Pt and Co ratios.

2.3 Physical characterization

Transmission electron microscope (TEM) images were investigated by FEI TECNAI F20 operated at 200 kV. The crystal structure of the catalysts was checked by X-ray diffraction (XRD) on a Bruker D8 Advance. The electronic structure information was recorded by X-ray photoelectron spectroscopy (XPS). The metal content of Pt_xCo/C was measured by inductively coupled plasma (ICP).

2.4 Electrochemical measurements

The electrochemical tests were performed on a CS300 electrochemical station with a standard three-electrode cell at room temperature. The working electrode was a rotating disk electrode (RDE). The active area of the electrode was 0.196 cm^2. The counter electrode was a Pt wire, and the reference electrode was a reversible hydrogen electrode (RHE). The electrolyte was 0.1 $mol\cdot L^{-1}$ $HClO_4$ aqueous solution. The cathode was prepared as follows: 30 mg sample, 5 ml ethanol, 5 ml ultrapure water and 120 μl 5 wt% Nafion were mixed thoroughly by ultrasonic method. 2 μl catalysts ink was pipetted on the clear glassy carbon disk. Cyclic voltammetry (CV) tests were recorded in N_2-saturated $HClO_4$ (0.1 $mol\cdot L^{-1}$) from 0.05 to 1.05 V at a scan rate of 50 $mV\cdot s^{-1}$. Liner scan voltammetry (LSV) tests were conducted in O_2-saturated $HClO_4$ (0.1 $mol\cdot L^{-1}$) at a scan rate of 5 $mV\cdot s^{-1}$ under 1600 $r\cdot min^{-1}$ between 0.30 and 1.05 V. The accelerated degradation tests (ADTs) were conducted at a sweep rate of 100 $mV\cdot s^{-1}$ from 0.6 to 1.2 V in N_2-saturated environment.

2.5 PEMFC single-cell tests

The single-cell tests were carried out in a fuel cell system. The Pt_3Co/C catalyst, isopropanol, ultrapure water and 5 wt% Nafion were mixed by ultrasonication to obtain the catalyst ink. Then, we sprayed the catalyst ink on one side of a Nafion 211 membrane as cathode. The commercial Pt/C was loaded to the anode. The Pt loadings were 200 and 400 $\mu g\cdot cm^{-2}$, respectively, at the cathode and anode. Membrane electrode assembly with an area of 5 cm^2 was fabricated by assembling a gas diffusion layer, anode and cathode. The temperature of the cell was controlled at 75 °C. The back pressures of the cathode and anode were 70 and 80 kPa, respectively. The anode was fed with humidified hydrogen and cathode with air.

3 Results and discussion

3.1 Composition, structure and morphology characterization

The real metal content of Pt$_x$Co/C catalysts was recorded by ICP, as shown in Table 1. The measured Pt/Co ratios for PtCo/C, Pt$_2$Co/C and Pt$_3$Co/C catalysts are 54:46, 69:31 and 76:24, respectively, which are approximately equal to the ideal values. The results demonstrate that the one-pot method is effective for preparation of Pt$_x$Co/C catalysts.

Figure 1 shows XRD patterns of Pt$_x$Co/C catalysts and commercial Pt/C catalyst. For Pt$_x$Co/C, obvious face-centered cubic (fcc) structure is indexed. The slight peak at $2\theta = 25°$ belongs to C(002) crystal plane, and the other four diffraction peaks at around 39.8°, 46.2°, 67.6° and 81.4° correspond to Pt(111), (200), (220) and (311) planes, respectively [40, 41]. Incorporating Co into Pt lattice would shorten Pt–Pt distance due to compressive strain. XRD patterns show that the platinum characteristic diffraction peaks of the Pt$_x$Co/C catalysts shift positively compared to those of commercial Pt/C, indicating the lattice shrinkage. Besides, the shift of the Pt peaks increases with Pt contents decreasing, demonstrating that a number of Co atoms are incorporated into the Pt lattice to form an alloy phase [42–44], which can be further confirmed by that no any characteristic peaks of pure Pt or Co are observed.

Figure 2 shows TEM morphologies of the Pt$_x$Co/C catalysts. It can be seen that Pt$_x$Co/C catalysts are evenly distributed on the surface of carbon support. The average particle diameters of PtCo/C, Pt$_2$Co/C and Pt$_3$Co/C are (3.45 ± 0.42), (3.92 ± 0.52) and (4.25 ± 0.88) nm, respectively. This indicates that the current synthesis method is available to obtain the Pt$_x$Co/C catalysts without adding any other surfactants.

3.2 XPS analysis

The electronic structure information of the Pt alloys with Co was investigated by XPS in Fig. 3. It can be seen that the Pt 4f peaks of Pt$_x$Co/C positively shift compared with Pt/C, which can be ascribed to the decrease in Pt–Pt distance caused by the electronic structure modification of Pt [45–47]. As is well known, the catalysts activity and durability are influenced by the chemical adsorption/desorption energy between oxygen species and Pt. The positive shift of Pt 4f spectra indicates that alloying Pt with Co would weaken the interaction between Pt and oxygen species. The influence benefits to expose more catalytic sites on the catalyst surface, leading to promoted catalysts electrocatalytic activity. The Pt 4f peaks of Pt-based catalysts can be splitted into two peaks, which are regarded as Pt 4f$_{5/2}$ and Pt 4f$_{7/2}$ [48, 49]. The binding energy of Pt 4f spectra for Pt$_x$Co/C and Pt/C is shown in Table 2. In terms of Pt$_3$Co/C, the peaks located at 71.62 (Pt 4f$_{7/2}$) and 75.00 eV (Pt 4f$_{5/2}$) are assigned to pure Pt^0, while the peaks located at 72.50 (Pt 4f$_{7/2}$) and 76.10 eV (Pt 4f$_{5/2}$) are attributed to Pt^{2+} species. The proportions of Pt^0 and Pt^{2+} are determined by XPS, showing that the metallic Pt^0 proportion (71.34%) of Pt$_3$Co/C on the surface is much higher than that of Pt/C (57.12%). Same phenomenon is observed for PtCo/C and Pt$_2$Co/C. It has been demonstrated that Pt^0 is the most active valence state of Pt for oxygen reduction reaction. The higher the proportion of Pt^0 is on the catalyst surface, the more the Pt catalytic sites are for oxygen reduction, which is the reason that as-prepared Pt$_x$Co/C catalysts exhibit remarkably improved kinetics for the cathodic reaction as compared with the commercial Pt/C catalyst. As shown in Fig. S1, the Co 2p$_{3/2}$ peak of Pt$_x$Co/C is located at around 780.0 eV, corresponding to Co^0. The Co^0 2p peak shows a positive shift in comparison with bulk Co (778.3 eV), confirming the electron donation from Co to Pt.

Table 1 Compositions of Pt$_x$Co/C catalysts

Catalyst	Nominal Pt:Co ratio (atomic)	Composition from ICP analysis
PtCo/C	1:1	54:46
Pt$_2$Co/C	2:1	69:31
Pt$_3$Co/C	3:1	76:24

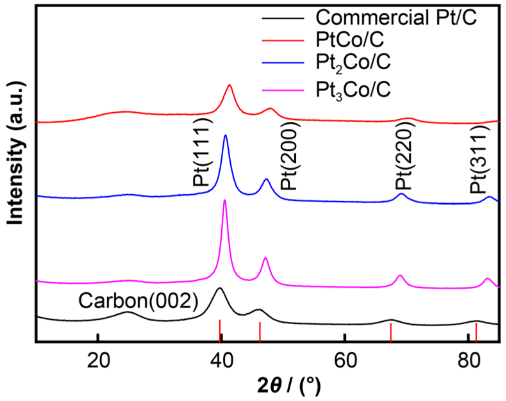

Fig. 1 XRD patterns of carbon-supported and Pt$_x$Co/C catalysts

3.3 Electrochemical performance

Electrocatalytic activities of Pt$_x$Co/C catalysts were assessed by CV and LSV tests by comparing with commercial Pt/C. In order to remove the impurities on the catalysts surface and activate the active sites of the

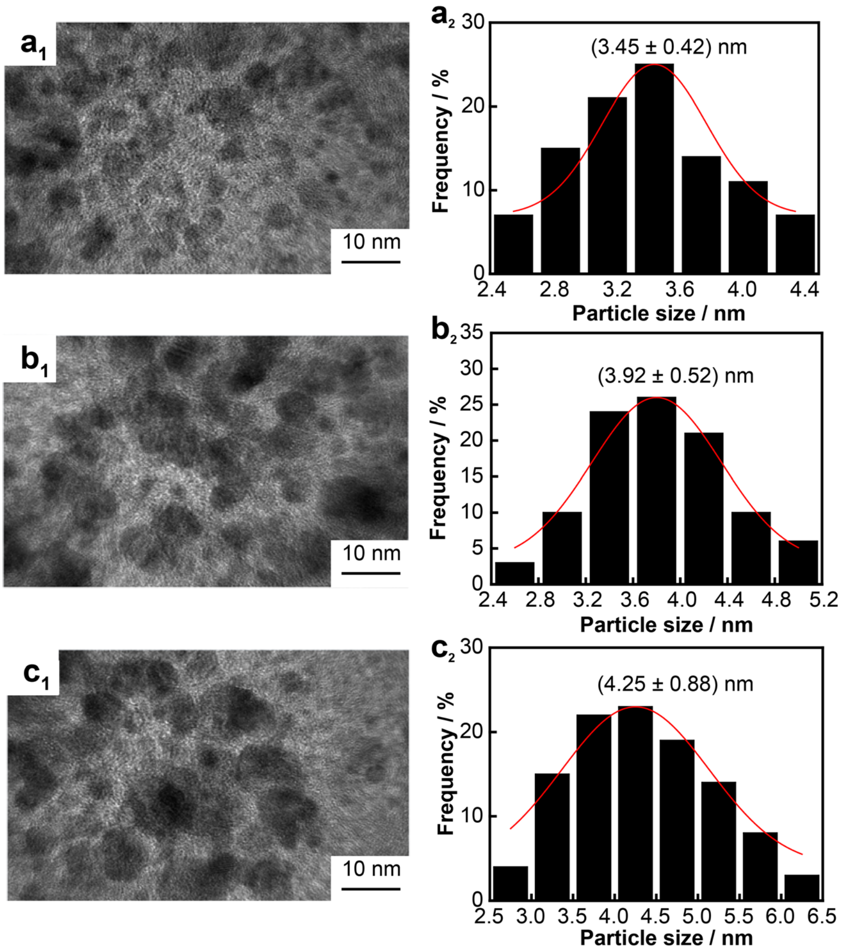

Fig. 2 TEM images and corresponding size distribution diagrams: **a_1, a_2** PtCo/C; **b_1, b_2** Pt_2Co/C; **c_1, c_2** Pt_3Co/C

catalysts, we scanned several cycles from 0.05 to 1.05 V before recording CV curves. The CV curves are shown in Fig. 4. The characteristic peaks in the potential between 0.05 and 0.50 V are assigned to the hydrogen adsorption/desorption on Pt (Fig. 4a), which we use to calculate the specific electrochemical surface area (ECSA). The specific electrochemical surface area (ECSA) was calculated from the following equation:

$$\mathrm{ECSA} = \frac{Q}{0.21 * m_{\mathrm{Pt}}} \tag{1}$$

where Q is the Coulombic charge associated with hydrogen desorption (mC), m_{Pt} is Pt loading (mg). The ECSA values are 74.48, 68.09 and 55.09 $m^2 \cdot g^{-1}$ for PtCo/C, Pt_2Co/C and Pt_3Co/C, respectively, which are lower than that of commercial Pt/C (80.46 $m^2 \cdot g^{-1}$), indicating that the size of nanoparticles has some influences on ECSA. The characteristic potential peak between 0.6 and 1.0 V is assigned to oxidation/reduction of Pt. For Pt_xCo/C, the peak at around 0.9 V is more positive than that of Pt/C. This phenomenon indicates that the bond between oxygen intermediate such as OH_{ad} or OOH_{ad} and Pt in the Pt_xCo/C catalysts is weaker, which is helpful to improve ORR catalytic activity. Figure 4b shows ORR polarization curves of Pt_xCo/C and commercial Pt/C catalysts. The half-wave potential ($E_{1/2}$) of PtCo/C, Pt_2Co/C and Pt_3Co/C are 907, 902 and 900 mV, higher than that of Pt/C (866 mV). This proves that alloying Pt with Co leads to improved ORR activity. To further evaluate electrocatalytic activities of the Pt_xCo/C and Pt/C catalysts, mass activities and specific activities at 0.9 V are calculated, as displayed in Table 3. The mass activities of PtCo/C, Pt_2Co/C and Pt_3Co/C are 0.526, 0.462 and 0.441 $A \cdot mg_{Pt}{}^{-1}$, which are, respectively, 2.60, 2.31 and 2.22 times higher than that of Pt/C (0.200 $A \cdot mg_{Pt}{}^{-1}$). The specific activities of PtCo/C, Pt_2Co/C and Pt_3Co/C are 706.59, 679.41 and 801.83 $\mu A \cdot cm^{-2}$, which are accordingly 2.89, 2.76 and 3.28 times higher than that of Pt/C (244.75 $\mu A \cdot cm^{-2}$). In addition, LSV curves of Pt_xCo/C at various rotation speeds and Koutechy-Levich (K-L) plots are shown in Fig. 4d. The Koutechý-Levich equation is as follows:

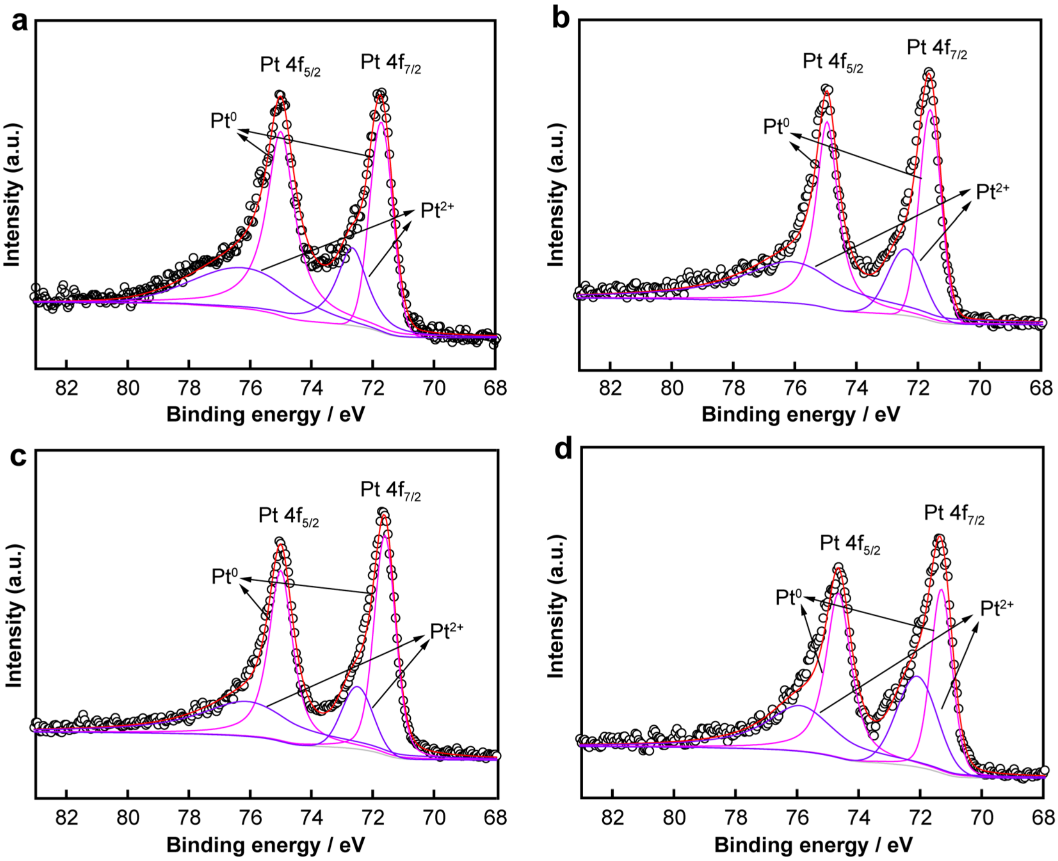

Fig. 3 XPS analysis for Pt 4f spectra: **a** Pt/C; **b** PtCo/C; **c** Pt_2Co/C; **d** Pt_3Co/C

Table 2 Binding energy (BE) of Pt 4f spectra and percentages of Pt^0 and Pt^{2+} in Pt_xCo/C and commercial Pt/C catalysts

Catalyst	Chemical state	Pt 4f$_{7/2}$ BE / eV	Pt 4f$_{5/2}$ BE / eV	Proportion / %
PtCo/C	Pt^0	71.72	75.03	66.24
	Pt^{2+}	72.67	76.20	33.76
Pt_2Co/C	Pt^0	71.60	74.95	68.16
	Pt^{2+}	72.43	76.13	31.84
Pt_3Co/C	Pt^0	71.62	75.00	71.34
	Pt^{2+}	72.50	76.10	28.66
Pt/C	Pt^0	71.33	74.65	57.12
	Pt^{2+}	72.10	75.93	42.88

$$\frac{1}{j}=\frac{1}{j_{\mathrm{k}}}+\frac{1}{j_{\mathrm{d}}}=\frac{1}{j_{\mathrm{k}}}+\frac{1}{0.62nFcD^{2/3}v^{-1/6}\omega^{1/2}} \qquad (2)$$

where j_{k} is kinetic current density, j_{d} is diffusion-limiting current density, n is the number of electrons transferred per oxygen molecule, F is Faraday constant (96,485 $C\cdot mol^{-1}$), c is O_2 concentration (1.26×10^{-6} $mol\cdot cm^{-3}$), D is oxygen diffusion coefficient in the electrolyte (1.9×10^{-5} $cm^2\cdot s^{-1}$), v is kinematic viscosity of the electrolyte solution (1.009×10^{-2} $cm^2\cdot s^{-1}$), and ω is the electrode rotation speed ($rad\cdot s^{-1}$). The K-L plots were calculated at different potentials from 0.8 to 0.9 V. The transfer numbers of PtCo/C, Pt_2Co/C and Pt_3Co/C are 3.99, 3.92 and 3.93, respectively, indicating that their oxygen reduction is $4e^-$ transfer reaction. The Tafel slopes that reflect the kinetics of electrochemical reactions were extracted from curves of Pt/C and Pt_xCo/C. As shown in Fig. S2, PtCo/C (87 $mV\cdot dec^{-1}$), Pt_2Co/C (91 $mV\cdot dec^{-1}$) and Pt_3Co/C (93 $mV\cdot dec^{-1}$) show lower Tafel slopes than Pt/C (96 $mV\cdot dec^{-1}$) in the low overpotential region (> 0.8 V), indicating that Pt_xCo/C catalysts show more beneficial kinetics.

The durability of Pt_xCo/C catalysts was evaluated by CV testing between 0.6 and 1.2 V (vs. RHE) in N_2-saturated environment. LSV curves were recorded after 5000 cycles, as shown in Fig. 5. After 5000 cycles, the half-wave potentials of PtCo/C, Pt_2Co/C, Pt_3Co/C and Pt/C negatively shift by 18, 30, 18, 6 mV, respectively; their mass activities decay 50.4%, 30.0%, 12.1% and 21.5% compared with the initial values; and their specific activities decay 45.6%, 28.0%, 18.1% and 30.2%. Among the Pt_xCo/C catalysts, Pt_3Co/C catalyst shows the highest activity and durability.

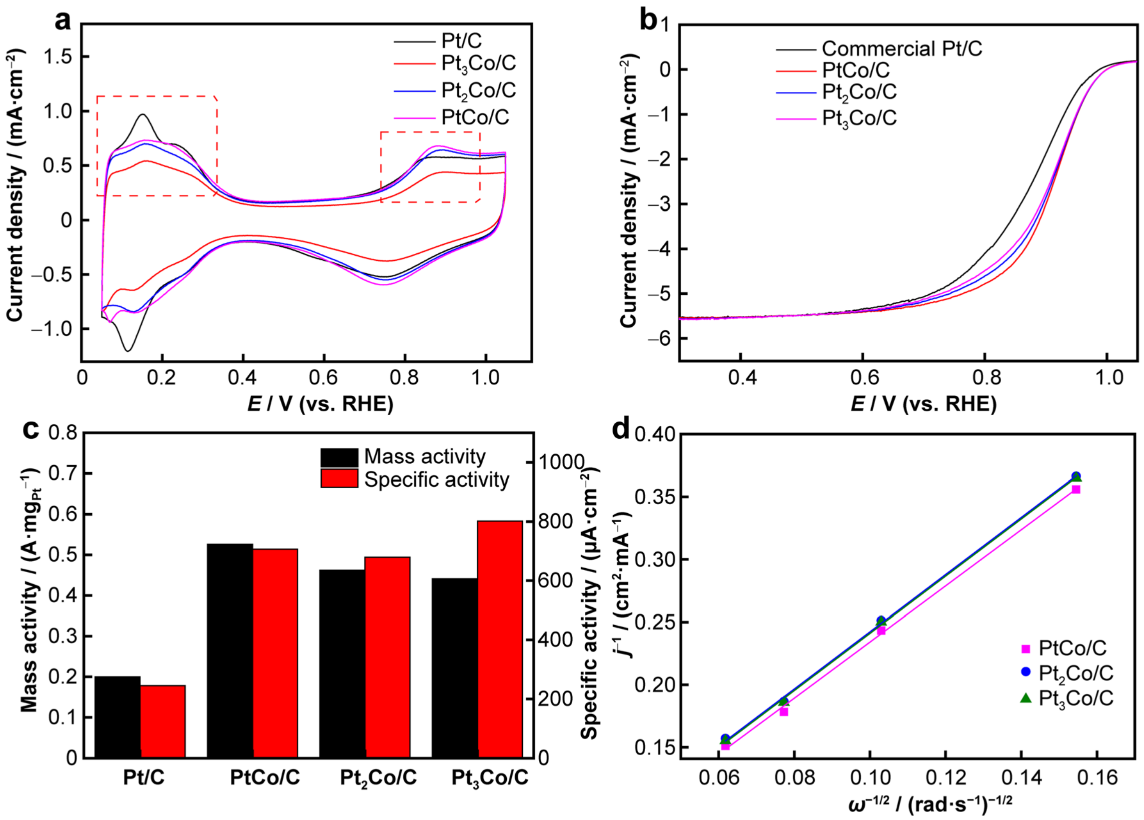

Fig. 4 **a** CV curves in N_2-saturated 0.1 mol·L^{-1} $HClO_4$ scanning at 50 mV·s^{-1}; **b** LSV curves in O_2-saturated 0.1 mol·L^{-1} $HClO_4$ scanning at 5 mV·s^{-1}; **c** mass and specific activities; **d** K-L plots of Pt_xCo/C and commercial Pt/C catalyst

Table 3 ORR activities of Pt_xCo/C and commercial Pt/C catalysts

Catalyst	$E_{1/2}$ / mV	ECSA / (m^2·g^{-1})	MA at 0.9 V / (A·mg$_{Pt}^{-1}$)	SA at 0.9 V / (μA·cm^{-2})
Pt/C	866	80.46	0.200	244.75
PtCo/C	907	74.48	0.526	706.59
Pt_2Co/C	902	68.09	0.462	679.41
Pt_3Co/C	900	55.09	0.441	801.83

3.4 PEMFC single-cell tests

We focused on Pt_3Co/C catalyst and further evaluated its electrocatalytic activity in a single cell by comparing with Pt/C catalyst. Figure 6a shows *I-V* curves of electrodes consisting Pt_3Co/C and Pt/C cathodes. Significantly, the maximum power density of the Pt_3Co/C electrode is 0.931 W·cm^{-2}, much higher than that of the Pt/C (0.834 W·cm^{-2}). The Pt loadings of Pt_3Co/C and Pt/C in cathode are 0.2 and 0.4 mg·cm^{-2}, respectively (Table 4). The *I-V* curves of the electrodes are normalized to the Pt loading for further comparation. The Pt_3Co/C shows superior maximum power density of 4.655 W·mg$_{Pt}^{-1}$, which is 2.23 times higher than that of the Pt/C (2.085 W·mg$_{Pt}^{-1}$).

4 Conclusion

In summary, we have successfully prepared a series of Pt_xCo/C catalysts by using a facile one-pot method without adding any surfactants. The as-obtained Pt_xCo/C nanoparticles are evenly distributed on the carbon support. All the Pt_xCo/C catalysts exhibit significantly improved mass activity and specific activity than the commercial Pt/C catalyst. Among them, Pt_3Co/C shows the best electrochemical performance and durability. Its maximum power density in air-H_2 fuel cell is 4.655 W·mg$_{Pt}^{-1}$, which is 2.23 times higher than that of Pt/C. The remarkable improvement on the enhanced ORR activity and durability is attributed to the change of the electronic structure on the surface Pt by alloying Pt with Co. We believe that the present work can provide an effective strategy to improve

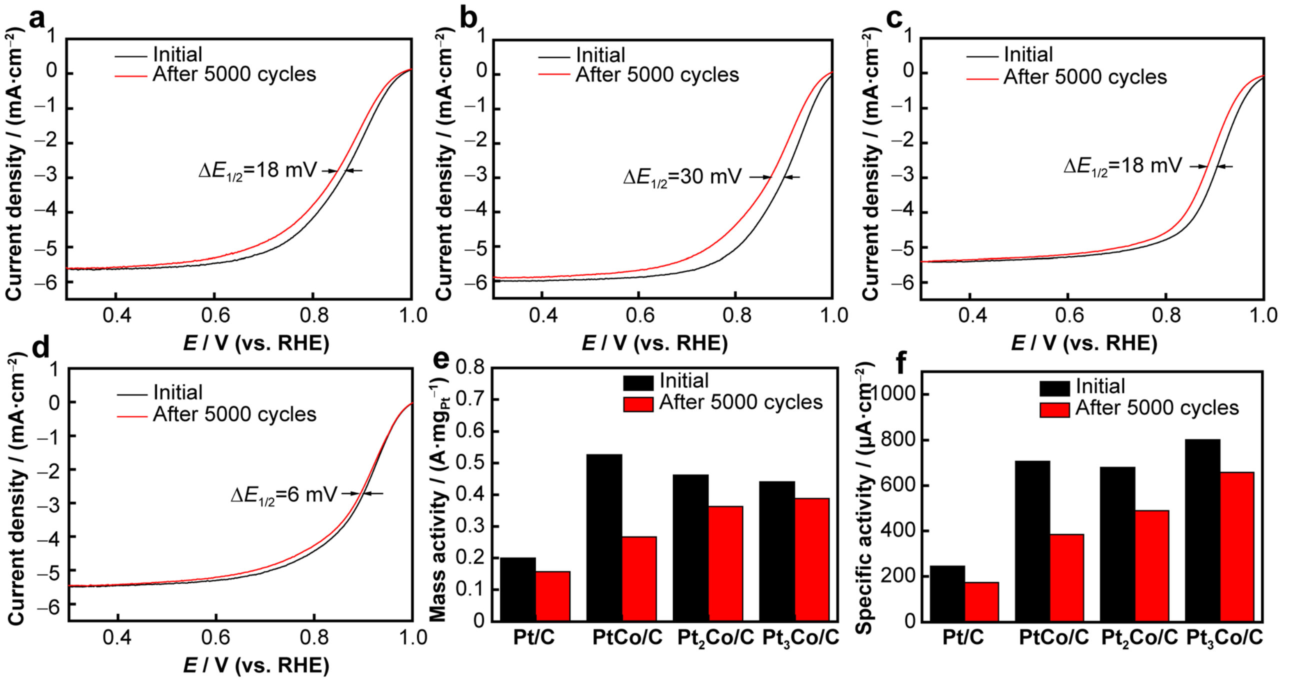

Fig. 5 LSV curves of **a** commercial Pt/C, **b** PtCo/C, **c** Pt_2Co/C, and **d** Pt_3Co/C; comparison of **e** mass activities and **f** specific activities between Pt_xCo/C and commercial Pt/C before and after 5000 cycles with scanning rate of 100 mV·s^{-1} in O_2-saturated 0.1 mol·L^{-1} $HClO_4$

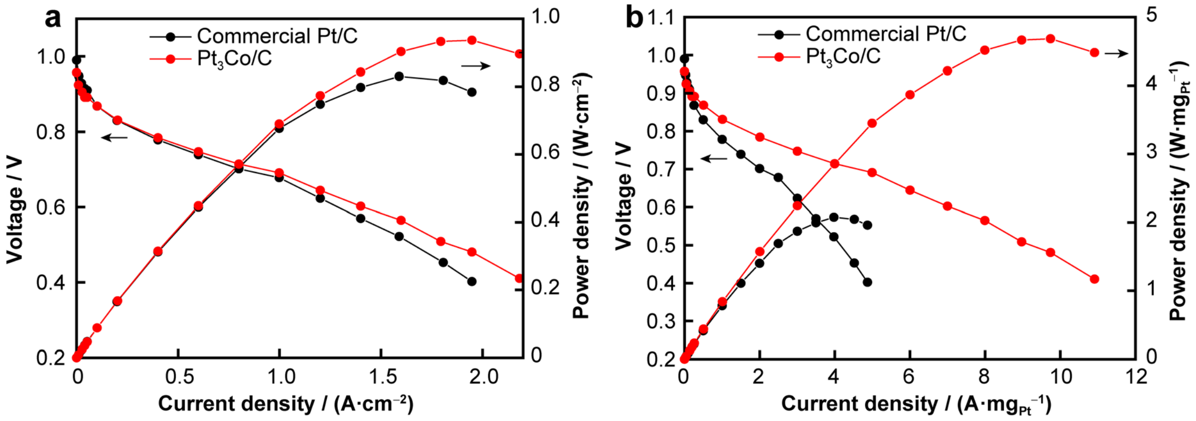

Fig. 6 **a** *I-V* curves of electrodes consisting Pt_3Co/C and commercial Pt/C based cathodes; **b** *I-V* curves with current density normalized to Pt loading

Table 4 Comparison between Pt_3Co/C and Pt/C based cathodes in single cell tests

Electrode	Pt loading / (mg·cm^{-2})	Maximum power density	
		W / cm^2	*W* / mg$_{Pt}$
Pt_3Co/C	0.2	0.931	4.655
Pt/C	0.4	0.834	2.085

the activity and durability of Pt-based catalysts for the commercialization of PEMFCs.

Acknowledgements This work was financially supported by the Project of National Natural Science Foundation of China (No. 5202780089).

Declarations

Conflict of interests The authors declare that they have no conflict of interest.

References

[1] Wang Y, Chen KS, Mishler J, Cho SC, Adroher XC. A review of polymer electrolyte membrane fuel cells: technology,

applications, and needs on fundamental research. Appl Energy. 2011;88(4):981. https://doi.org/10.1016/j.apenergy.2010.09.030.

[2] Debe MK. Electrocatalyst approaches and challenges for automotive fuel cells. Nature. 2012;486(7401):43. https://doi.org/10.1038/nature11115.

[3] Wang XX, Swihart MT, Wu G. Achievements, challenges and perspectives on cathode catalysts in proton exchange membrane fuel cells for transportation. Nat Catal. 2019;2(7):578. https://doi.org/10.1038/s41929-019-0304-9.

[4] Ferreira PJ, la O' GJ, Shao-Horn Y, Morgan D, Makharia R, Kocha S, Gasteiger HA. Instability of Pt/C electrocatalysts in proton exchange membrane fuel cells: a mechanistic investigation. J Electrochem Soc. 2005;152(11):A2256. https://doi.org/10.1149/1.2050347.

[5] Nadeem M, Wan YH, Xia CR. The effect of group IIIA oxides on the oxygen reduction reaction at cathodes for intermediate-temperature solid oxide fuel cells. Compos B Eng. 2020;189: 107924. https://doi.org/10.1016/j.compositesb.2020.107924.

[6] Xu XY, Zhao J, Li MR, Zhuang LZ, Zhang JX, Aruliah S, Liang FL, Wang H, Zhu ZH. Sc and Ta-doped $SrCoO_3$-delta perovskite as a high-performance cathode for solid oxide fuel cells. Compos B Eng. 2019;178: 107491. https://doi.org/10.1016/j.compositesb.2019.107491.

[7] Liu B, Jia LC, Chi B, Pu J, Li J. A novel $PrBaCo_2O_{5+\sigma}$ $BaZr_{0.1}Ce_{0.7}Y_{0.1}Yb_{0.1}O_3$ composite cathode for proton-conducting solid oxide fuel cells. Compos B Eng. 2020;191: 107936. https://doi.org/10.1016/j.compositesb.2020.107936.

[8] Coleman EJ, Chowdhury MH, Co AC. Insights into the oxygen reduction reaction activity of Pt/C and PtCu/C catalysts. ACS Catal. 2015;5(2):1245. https://doi.org/10.1021/cs501762g.

[9] Venarusso LB, Sato RH, Fiorito PA, Maia G. Platinum systems electrodeposited in the presence of iron or palladium on a gold surface effectively catalyze oxygen reduction reaction. J Phys Chem C. 2013;117(15):7540. https://doi.org/10.1021/jp311343w.

[10] Wang YJ, Zhao NN, Fang BZ, Li H, Bi XTT, Wang HJ. Carbon-supported Pt-based alloy electrocatalysts for the oxygen reduction reaction in polymer electrolyte membrane fuel cells: particle size, shape, and composition manipulation and their impact to activity. Chem Rev. 2015;115(9):3433. https://doi.org/10.1021/cr500519c.

[11] Zhu YG, Shang CQ, Wang ZY, Zhang JQ, Yang MY, Cheng H, Lu ZG. Co and N co-modified carbon nanotubes as efficient electrocatalyst for oxygen reduction reaction. Rare Met. 2021; 40(1):90. https://doi.org/10.1007/s12598-019-01270-x.

[12] Fan MM, Liao DK, Aboud FMA, Shakir I, Xu YX. A universal strategy toward ultrasmall hollow nanostructures with remarkable electrochemical performance. Angew Chem Int Ed. 2020; 59(21):8247. https://doi.org/10.1002/anie.202000352.

[13] Xu H, Ding LX, Feng JX, Li GR. $Pt/Ni(OH)_2$-NiOOH/Pd multi-walled hollow nanorod arrays as superior electrocatalysts for formic acid electrooxidation. Chem Sci. 2015;6(12):6991. https://doi.org/10.1039/c5sc02544c.

[14] Bai XX, Geng JR, Zhao S, Li HX, Li FJ. Tunable hollow Pt@Ru dodecahedra via galvanic replacement for efficient methanol oxidation. ACS Appl Mater Interfaces. 2020;12(20):23046. https://doi.org/10.1021/acsami.0c06460.

[15] Li MF, Zhao ZP, Cheng T, Fortunelli A, Chen CY, Yu R, Zhang QH, Gu L, Merinov BV, Lin ZY, Zhu EB, Yu T, Jia QY, Guo JH, Zhang L, Goddard WA, Huang Y, Duan XF. Ultrafine jagged platinum nanowires enable ultrahigh mass activity for the oxygen reduction reaction. Science. 2016;354(6318):1414. https://doi.org/10.1126/science.aaf9050.

[16] Huang HW, Li K, Chen Z, Luo LH, Gu YQ, Zhang DY, Ma C, Si R, Yang JL, Peng ZM, Zeng J. Achieving remarkable activity and durability toward oxygen reduction based on ultrathin Rh-doped Pt nanowires. J Am Chem Soc. 2017;139(24):8152. https://doi.org/10.1021/jacs.7b01036.

[17] Gong MX, Deng ZP, Xiao DD, Han LL, Zhao TH, Lu Y, Shen T, Liu XP, Lin RQ, Huang T, Zhou GW, Xin HL, Wang DL. One-nanometer-thick Pt_3Ni bimetallic alloy nanowires advanced oxygen reduction reaction: integrating multiple advantages into one catalyst. ACS Catal. 2019;9(5):4488. https://doi.org/10.1021/acscatal.9b00603.

[18] Becknell N, Kang YJ, Chen C, Resasco J, Kornienko N, Guo JH, Markovic NM, Somorjai GA, Stamenkovic VR, Yang PD. Atomic structure of Pt_3Ni nanoframe electrocatalysts by in situ X-ray absorption spectroscopy. J Am Chem Soc. 2015;137(50): 15817. https://doi.org/10.1021/jacs.5b09639.

[19] Gong MX, Xiao DD, Deng ZP, Zhang R, Xia WW, Zhao TH, Liu XP, Shen T, Hu YZ, Lu Y, Zhao X, Xin HL, Wang DL. Structure evolution of PtCu nanoframes from disordered to ordered for the oxygen reduction reaction. Appl Catal B Environ. 2021;282:119617. https://doi.org/10.1016/j.apcatb.2020.119617.

[20] Zhu XX, Huang L, Wei M, Tsiakaras P, Shen PK. Highly stable Pt-Co nanodendrite in nanoframe with Pt skin structured catalyst for oxygen reduction electrocatalysis. Appl Catal B. 2021;281:119460. https://doi.org/10.1016/j.apcatb.2020.119460.

[21] Lim B, Jiang MJ, Camargo PHC, Cho EC, Tao J, Lu XM, Zhu YM, Xia YN. Pd-Pt bimetallic nanodendrites with high activity for oxygen reduction. Science. 2009;324(5932):1302. https://doi.org/10.1126/science.1170377.

[22] Kwon H, Kabiraz MK, Park J, Oh A, Baik H, Sl C, Lee K. Dendrite-embedded platinum-nickel multiframes as highly active and durable electrocatalyst toward the oxygen reduction reaction. Nano Lett. 2018;18(5):2930. https://doi.org/10.1021/acs.nanolett.8b00270.

[23] Chung DY, Yoo JM, Sung YE. Highly durable and active Pt-based nanoscale design for fuel-cell oxygen-reduction electrocatalysts. Adv Mater. 2018;30(42):1704123. https://doi.org/10.1002/adma.201704123.

[24] Wang Q, Zhao ZL, Zhang Z, Feng TL, Zhong RY, Xu H, Pantelides ST, Gu M. Sub-3 nm intermetallic ordered Pt_3In clusters for oxygen reduction reaction. Adv Sci. 2020;7(2): 1901279. https://doi.org/10.1002/advs.201901279.

[25] Chung DY, Jun SW, Yoon G, Kwon SG, Shin DY, Seo P, Yoo JM, Shin H, Chung YH, Kim H, Mun BS, Lee KS, Lee NS, Yoo SJ, Lim DH, Kang K, Sung YE, Hyeon T. Highly durable and active PtFe nanocatalyst for electrochemical oxygen reduction reaction. J Am Chem Soc. 2015;137(49):15478. https://doi.org/10.1021/jacs.5b09653.

[26] Puangsombut P, Tantavichet N. Effect of plating bath composition on chemical composition and oxygen reduction activity of electrodeposited Pt-Co catalysts. Rare Met. 2019;38(2):95. https://doi.org/10.1007/s12598-018-1082-2.

[27] Song GT, Wang Y, Qi Y, Li WM, Zhang LX. Fabrication of titanium nitride nanoparticles onto carbon nanotubes by atomic layer deposition for utilization as Pt electrocatalyst supports. Rare Met. 2020;39(7):784. https://doi.org/10.1007/s12598-019-01284-5.

[28] Gong QH, Wang LP, Yang N, Tian L, Xie G, Li B. Ternary PtSmCo NPs electrocatalysts with enhanced oxygen reduction reaction. J Rare Earths. 2020;38(12):1305. https://doi.org/10.1016/j.jre.2019.11.016.

[29] Vinayan BP, Jafri RI, Nagar R, Rajalakshmi N, Sethupathi K, Ramaprabhu S. Catalytic activity of Platinum-cobalt alloy nanoparticles decorated functionalized multiwalled carbon nanotubes for oxygen reduction reaction in PEMFC. Int J Hydrog Energy. 2012;37(1):412. https://doi.org/10.1016/j.ijhydene.2011.09.069.

[30] Lee KS, Jeon TY, Yoo SJ, Park IS, Cho YH, Kang SH, Choi KH, Sung YE. Effect of PtRu alloying degree on electrocatalytic activities and stabilities. Appl Catal B. 2011;102:334. https://doi.org/10.1016/j.apcatb.2010.12.023.

[31] Du XX, He Y, Wang XX, Wang JN. Fine-grained and fully ordered intermetallic PtFe catalysts with largely enhanced catalytic activity and durability. Energy Environ Sci. 2016;9(8):2623. https://doi.org/10.1039/c6ee01204c.

[32] Seo A, Lee J, Han K, Kim H. Performance and stability of Pt-based ternary alloy catalysts for PEMFC. Electrochim Acta. 2006;52(4):1603. https://doi.org/10.1016/j.electacta.2006.03.097.

[33] Gasteiger HA, Kocha SS, Sompalli B, Wagner FT. Activity benchmarks and requirements for Pt, Pt-alloy, and non-Pt oxygen reduction catalysts for PEMFCs. Appl Catal B. 2005;56:9. https://doi.org/10.1016/j.apcatb.2004.06.021.

[34] Lai WH, Zhang BW, Hu ZP, Qu XM, Jiang YX, Wang YX, Wang JZ, Liu HK, Chou SL. The Quasi-Pt-allotrope catalyst: hollow PtCo@Single-Atom Pt-1 on nitrogen-doped carbon toward superior oxygen reduction. Adv Funct Mater. 2019;29(13):1807340. https://doi.org/10.1002/adfm.201807340.

[35] Xia BY, Wu HB, Li N, Yan Y, Lou XW, Wang X. One-pot synthesis of Pt-Co alloy nanowire assemblies with tunable composition and enhanced electrocatalytic properties. Angew Chem Int Ed. 2015;54(12):3797. https://doi.org/10.1002/anie.201411544.

[36] Liu YX, Zhao GF, Wang DS, Li YD. Heterogeneous catalysis for green chemistry based on nanocrystals. Natl Sci Rev. 2015;2(2):150. https://doi.org/10.1093/nsr/nwv014.

[37] Wu BH, Zheng NF. Surface and interface control of noble metal nanocrystals for catalytic and electrocatalytic applications. Nano Today. 2013;8(2):168. https://doi.org/10.1016/j.nantod.2013.02.006.

[38] Kim C, Kim SS, Yang S, Han JW, Lee H. In situ shaping of Pt nanoparticles directly over grown on carbon supports. Chem Commun. 2012;48:6396. https://doi.org/10.1039/C2CC33126H.

[39] Kim HJ, Ruqia B, Kang MS, Lim SB, Choi R, Nam KM, Seo WS, Lee G, Choi SI. Shape-controlled Pt nanocubes directly grown on carbon supports and their electrocatalytic activity toward methanol oxidation. Sci Bull. 2017;62(13):943. https://doi.org/10.1016/j.scib.2017.05.029.

[40] Du ZK, Wang YL, Li JS, Liu JP. Facile fabrication of Pt–Ni alloy nanoparticles supported on reduced graphene oxide as excellent electrocatalysts for hydrogen evolution reaction in alkaline environment. J Nanopart Res. 2019;21(1):13. https://doi.org/10.1007/s11051-018-4436-7.

[41] Hu CG, Cao YX, Yang L, Bai ZY, Guo YM, Wang K, Xu PL, Zhou JG. Preparation of highly dispersed Pt-SnO$_x$ nanoparticles supported on multi-walled carbon nanotubes for methanol oxidation. Appl Surf Sci. 2011;257(18):7968. https://doi.org/10.1016/j.apsusc.2011.04.010.

[42] Travitsky N, Ripenbein T, Golodnitsky D, Rosenberg Y, Burshtein L, Peled E. Pt-, PtNi-, PtCo-supported catalysts for oxygen reduction in PEM fuel cells. J Power Sources. 2006;161(2):782. https://doi.org/10.1016/j.jpowsour.2006.05.035.

[43] Antolini E. Formation of carbon-supported PtM alloys for low temperature fuel cells: a review. Mater Chem Phys. 2003;78(3):563. https://doi.org/10.1016/S0254-0584(02)00389-9.

[44] Jayasayee K, Van Veen JAR, Manivasagam TG, Celebi S, Hensen EJM, de Bruijn FA. Oxygen reduction reaction (ORR) activity and durability of carbon supported PtM (Co, Ni, Cu) alloys: influence of particle size and non-noble metals. Appl Catal B Environ. 2012;111:515. https://doi.org/10.1016/j.apcatb.2011.11.003.

[45] Kang YS, Choi D, Park HY, Yoo SJ. Tuning the surface structure of PtCo nanocatalysts with high activity and stability toward oxygen reduction. J Ind Eng Chem. 2019;78:448. https://doi.org/10.1016/j.jiec.2019.05.021.

[46] Choi J, Cho J, Roh CW, Kim BS, Choi MS, Jeong H, Ham HC, Lee H. Au-doped PtCo/C catalyst preventing Co leaching for proton exchange membrane fuel cells. Appl Catal B. 2019;247:142. https://doi.org/10.1016/j.apcatb.2019.02.002.

[47] Tang XJ, Fang DH, Qu LJ, Xu DY, Qin XP, Qin BW, Song W, Shao ZG, Yi BL. Carbon-supported ultrafine pt nanoparticles modified with trace amounts of cobalt as enhanced oxygen reduction reaction catalysts for proton exchange membrane fuel cells. Chin J Catal. 2019;40(4):504. https://doi.org/10.1016/S1872-2067(19)63304-8.

[48] Yang WH, Zou LL, Huang QH, Zou ZQ, Hu YM, Yang H. Lattice contracted ordered intermetallic core-shell PtCo@Pt nanoparticles: synthesis, structure and origin for enhanced oxygen reduction reaction. J Electrochem Soc. 2017;164(6):H331. https://doi.org/10.1149/2.0851706jes.

[49] Luo BM, Xu S, Yan XB, Xue QJ. PtNi alloy nanoparticles supported on polyelectrolyte functionalized grapheneas effective electrocatalysts for methanol oxidation. J Electrochem Soc. 2013;160(4):F262. https://doi.org/10.1149/2.056303jes.